Electronic Supplementary Material (ESI) for Physical Chemistry Chemical Physics.

Supplementary Information for

Nature of Hydrated Proton Vibrations Revealed by Nonlinear Spectroscopy of Acid Water Nanodroplets

Oleksandr O. Sofronov and Huib J. Bakker*
AMOLF, Science Park 104, 1098 XG Amsterdam, The Netherlands
*h.bakker@amolf.nl

Contents

1. Experimental methods

We measured linear infrared absorption spectra in transmission geometry using a commercial Fourier transform spectrometer (Bruker Vertex 80v). We performed polarization resolved two-color mid-infrared pump-probe experiments using a home-built set up with two independently tunable optical parametric amplifiers (OPA). A regenerative Ti:sapphire amplifier (Coherent) provides 800 nm pulses (3.3 mJ, 35 fs) with a repetition rate of 1 kHz. A fraction of 1 mJ of this pulse energy is used to pump the first OPA. In this OPA, white light is generated by focusing a small fraction of the beam on a sapphire crystal. A spectral fraction of this white light was amplified by the rest of the 800 nm light in two parametric amplification process in a β-barium borate (BBO) crystal, yielding signal and idler pulses with a total energy of ~220 μJ. Subsequently, the signal and idler pulses are mixed in a silver gallium disulfide (AGS) crystal to generate mid-IR pulses at their difference frequency tunable from 2000 to 3500 cm^{-1} (1.3-4 μJ, 60 fs, fwhm=250 cm^{-1}). The obtained mid-IR beam was transmitted through a germanium plate to remove the residual signal and idler light and split by a wedged zinc selenide plate into probe and reference beams. The probe is sent through a time delay stage and focused into the sample where it spatially overlaps with the pump beam. The reference beam is also focused into the sample but not overlapping with the pump.

The pump pulses were generated by another OPA that is pumped by the remaining 2.3 mJ of 800 nm light. This OPA contains three amplification steps in two BBO crystals, and provides signal and idler pulses with a total energy of ~700 μJ. Mixing of signal and idler in an AGS crystal produces mid-IR pulses (20 μJ, 100 fs, fwhm=150 cm^{-1}) tunable in the range 2200-2700 cm^{-1}.

The polarization of the pump was set at 45° with respect to the probe with a half-wave plate. The energies of the pump and probe pulses at the sample position were 12 μJ (~60 GW/cm^2 peak power flux) and 0.2-0.5 μJ (~5-12 GW/cm^2 peak power flux) respectively, and the diameters of the focal spots of the pump and probe beams were ~250 μm and ~150 μm respectively. After the sample either the polarization component of the probe parallel or the polarization component perpendicular to the polarization of the pump was selected with a rotating wire-grid polarizer. The selected polarization component of the probe beam and the reference beam are both dispersed by a monochromator, and subsequently detected by two lines of each 32 pixels of a mercury-cadmium-telluride (MCT) detector array. The probe signal detected by each pixel is normalized to the reference signal of the corresponding pixel to correct for pulse-to-pulse fluctuations in energy and spectrum.

The transient absorption signal is obtained by mechanically chopping every second pump pulse, and by comparing the transmission of the probe with pump to the transmission without pump. Due to artifacts at pump-probe time overlap, we analyze the transient spectra only for delay times ≥0.25 ps.

The measurements of the anisotropy dynamics when pumping and probing at 2600 cm^{-1} were performed with a different pump-probe setup that allows for an even better signal-to-noise ratio as a result of a different scheme of generating the mid-infrared pump and probe pulses. In that setup an Yb-medium based laser (Light Conversion) pumps a commercial OPA, that directly generates an idler pulse with a central frequency of 2600 cm^{-1} (12 μJ, 200 fs, fwhm=100 cm^{-1}).

This beam was split into pump, probe and reference beams, which were used in a pump-probe setup identical to the setup described above. The energies of the pump and probe pulses at the sample position were 5 μJ (~13 GW/cm^2 peak power flux) and 0.2 μJ (~1.5 GW/cm^2 peak power flux) respectively, and the diameters of the focal spots of the pump and probe beams were ~250 μm and ~150 μm respectively.

For precise anisotropy measurements we checked that the pump power transmitted through the rotating polarizer in perpendicular polarization configuration is <2% of the pump power transmitted in parallel polarization configuration. From the spectra measured in parallel and perpendicular polarization we construct the isotropic signal $\Delta\alpha_{iso}=(\Delta\alpha_{\parallel} + 2\Delta\alpha_{\perp})/3$ and the anisotropy $R=(\Delta\alpha_{\parallel} - \Delta\alpha_{\perp})/(\Delta\alpha_{\parallel} + 2\Delta\alpha_{\perp})$. We averaged the data measured at different frequencies around 2250, 2300 or 2600 cm^{-1} (15 pixels, ±50 cm^{-1} for the two-color setup and 6 pixels, ±20 cm^{-1} for the one-color setup from the central frequency). The error bars of the data points represent the standard deviation of the anisotropy over different pixels. The averaged data were fit by exponential functions from 0.4 ps to 2.5 (AOT reverse micelles) or from 0.4 ps to 4 ps (CTAB reverse micelles). From the fits we also extract the anisotropy value R_0 at zero delay time.

All used chemicals were purchased from Sigma-Aldrich. Cationic nanodroplets were prepared as described before.[1] Cetyltrimethylammonium bromide (CTAB) and 1-hexanol (99%, anhydrous) were dissolved in n-hexane (99%, anhydrous) at concentrations of 0.11 M and 0.61 M, which yields a ratio [hexanol]:[CTAB]=3:1 in the micellar phase. By adding water (ultrapure milli-Q grade) and hydrobromic acid (HBr, 48%) we varied the hydration ratio $w_0=([H_2O]+[HBr])/[CTAB]$ from 8 to 40 with a constant HBr concentration of 7 M in the aqueous phase. This procedure yields nearly spherical nanodroplets with a water pool diameter $d_w=0.19\times w_0$. Anionic microemulsions were prepared by dissolving sodium dioctylsulfosuccinate (AOT, 99%) in carbon tetrachloride (CCl_4, 99.5%, anhydrous) at a concentration of 0.5 M. Water and perchloric acid ($HClO_4$, 70%) were added to achieve a ratio $w_0=([H_2O]+[HClO_4])/[AOT]$ ranging from 1 to 3 and a $HClO_4$ concentrations in aqueous phase of 7.2 M (w_0=1; 1.5; 2) or 4.8 M (w_0=2; 2.5; 3). The used sodium dioctylsulfosuccinate (AOT), originally contained water ($[H_2O]$:[AOT]=0.4), which was taken into account when preparing the samples. These mixtures were kept in an ultrasonic bath for 1.5 hour to completely equilibrate the microemulsions, as evidenced by their complete transparency. We could not equilibrate anionic microemulsions with w_0>3 or containing other acids (HBr, HCl, CF_3SO_3H), even when the acid concentrations was lowered to 3 M. In a recent study we investigated the effect of the acid concentration on the anisotropy dynamics of the hydrated proton for solutions of HBr in water, and found that the concentration does not lead to significant changes in these dynamics within a concentration range 0.5-7 M.[1] This finding implies that in this concentration range the anion Br^- has very little effect on the spectral response and transfer dynamics of the hydrated protons. Because of the relatively low vibrational cross-sections of the hydrated protons it is not possible to measure the vibrational spectrum of the hydrated proton in solution at much lower concentration.

The AOT microemulsions were stable for 4-7 days after preparation. After that time the nanodroplets were observed to aggregate and the mixtures became opaque. All the measurements on AOT microemulsions were thus done within two days after their preparation. In both the

FTIR and the pump-probe measurements, the samples were kept between two 2 mm thick calcium fluoride (CaF_2) windows, separated by a 50-200 μm PTFE spacer.

2. Size of the nanodroplets

The size of anionic reverse micelles may change upon the addition of acid, as we observed before for cationic reverse micelles.[1] To test this we performed pump-probe experiments for neat water nanodroplets and acidic water nanodroplets measuring the excited state relaxation dynamics of the water OH-stretch vibrations. The OH-stretch relaxation rate was shown to be dependent on the size of water/AOT reverse micelles and can thus be used to estimate the diameter of the nanodroplets.[2] In Figure S1A we show the transient absorption spectra for acidic water nanodroplet (w_0=1) following excitation at 3470 cm^{-1} (frequency of the maximum of the water OH-stretch absorption). At short delay times the spectra consist of a negative absorption change above ~3350 cm^{-1} due to bleaching of the fundamental v=0→1 transition and a positive absorption change at lower frequency, due to v=1→2 excited state absorption. At long delay times (>5 ps) the spectrum consists only of a negative absorption change at high frequency due to heating of water molecules following the vibrational relaxation. Subsequently, the heat is transferred to the surfactant molecules and oil phase, which results in a decrease of this heating signal.

The spectral dynamics at frequencies <3300 cm^{-1} is determined only by the vibrational relaxation of the excited OH-stretch vibrations, i.e. it represents the vibrational relaxation rate. In Figure S1B we compare the transient absorption dynamics at 3200 cm^{-1} for neat (lines) and acidic (dots) water nanodroplets of different w_0. We see that the vibrational relaxation becomes faster with increasing water content, which indicates that the size of the nanodroplets increases.[2] Also we observe that the relaxation rate in the acidic water nanodroplets is exactly the same as in the neat water nanodroplets of the same w_0. From this we conclude that the size of the nanodroplets does not change with the addition of acid. Using the results of earlier studies,[2,3] the diameters d_w of the water nanodroplets contained in AOT reverse micelles with w_0=1, 2, and 3, are 1.1, 1.5, and 1.8 nm, respectively. For cationic CTAB reverse micelles we have found that d_w=0.19×w_0, which implies that a CTAB/hexanol reverse micelle with w_0=12 will have approximately the same size (d_w=2.2 nm) as an AOT micelle with w_0=3.

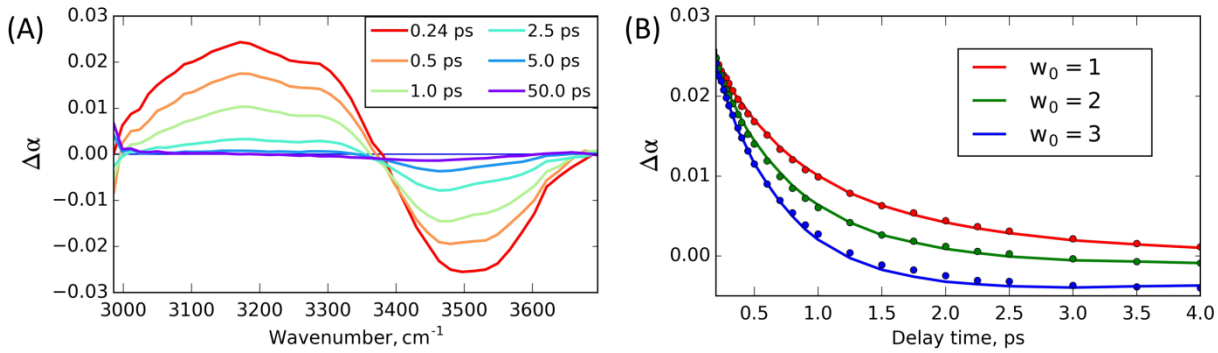

Figure S1. (A) Isotropic transient absorption spectra mesaured for the $HClO_4$/water/AOT system with w_0=1 following excitation at 3470 cm^{-1}. (B) Isotropic transient absorption dynamics probed at 3200 cm^{-1} for different acidic (dots) and neat water (lines) AOT reverse micelles.

3. Transient spectra of the hydrated protons in the anionic reverse micelles

In Figure S2 we show isotropic transient spectra at different pump-probe delay times following excitation of the OH-stretch vibrations of proton solvation structures at 2600 cm^{-1} for three different sizes of AOT reverse micelles. At all delay times the spectra show a broad negative absorption change in the frequency range from 2000 cm^{-1} to 3500 cm^{-1} and a small positive absorption change in the frequency range from 3500 cm^{-1} to 3600 cm^{-1}. The spectral region 2850-3000 cm^{-1} is not accessible due to strong absorption of the CH-stretch vibrations of the surfactant. The spectrum can be subdivided into two frequency regions: 2000-2850 cm^{-1} and 3000-3600 cm^{-1}. The low-frequency part of the spectrum represents the OH-stretch vibrations in the core of the hydrated proton, and the high-frequency part represents the response of the OH stretch vibrations of water molecules in the outer solvation shells of the proton, and of water molecules not interacting with protons.[4]

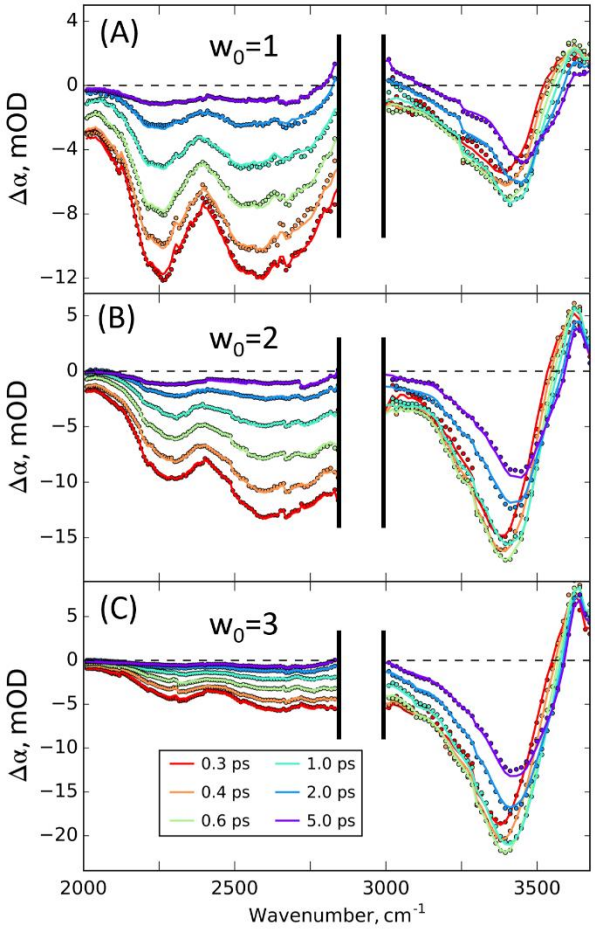

Figure S2. Isotropic transient spectra of acidic water AOT nanodroplets of different sizes following excitation with an intense mid-infrared pump pulse centered at 2600 cm^{-1}. The lines represent results of fits to the kinetic model described in the text.

Due to nonresonant artifacts from the CaF_2 windows, we cannot determine the response of the OH vibrations at delay times <0.3 ps. To check if other transient spectral components appear at short delay times, we also measured pump-probe spectra of $HClO_4/H_2O$/AOT/CCl_4 systems using a sample cell with 500 nm thick silicon nitride membranes instead of calcium fluoride windows. Because of their small thickness, the nonresonant signal of these silicon nitride membrane at short delay times is negligibly small. Hence, the signal at early delay times will only show coherent artifacts due to the sample itself. This allows us to measure transient spectra at delay times down to 150 fs. As we see in Figure S3, the transient spectra in the range of 0.15-0.3 ps are qualitatively the same as the spectra shortly after 0.3 ps. The spectra contain oscillatory components between 2400 and 2800 cm^{-1} which are the result of the interference of the probe with probe light that is two times reflected by the ultrathin Si_3N_4 membrane of the sample cell.

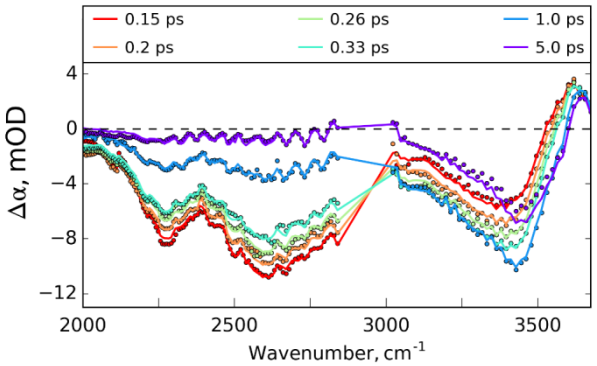

Figure S3. Isotropic transient spectra of acidic water AOT nanodroplets (w_0=2) following excitation with an intense mid-infrared pump pulse centered at 2600 cm^{-1} measured with the silicon nitride sample cell described in the text.

In the 3000-3600 cm^{-1} spectral region we observe a fast growth of a negative band (until ~0.6 ps) and a shift of this band to higher frequencies. These spectral dynamics can be explained from energy transfer from the core of the excited proton hydration structure to its outer shells. The OH-stretch vibrations of the hydrated proton excited by the pump pulse relax to the ground state within 100 fs by transferring their vibrational energy to low-frequency hydrogen-bond modes.[5,6] This process corresponds to strong heating of the local environment of the initially excited vibration. Subsequently, the excess energy equilibrates between the inner and outer solvation shells, which leads to the rise of a signal corresponding to the creation of hot water molecules in the outer hydration shells. These latter water molecules absorb at 3000-3600 cm^{-1} and due to the heating effect their absorption decreases, thus explaining the observation of a negative transient absorption signal in this frequency region.

We model the isotropic spectral dynamics with a three-level cascade model. The first state relaxes exponentially and populates the second state, which also relaxes exponentially to populate the third state. The extracted spectral components and the time constants are shown in Figure S4. The result of the fit is shown by the lines in Figure S2.

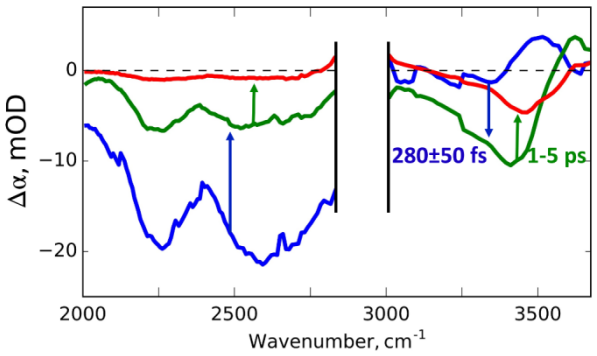

Figure S4. Transient spectral components extracted from the fit of transient spectra of w_0=1 nanodroplets. The component shown in blue converts into the component shown in green with time constant 280±50 fs, and the green subsequently converts into the spectrum shown in red with nonexponential picosecond dynamics.

We find that in the range of 0.3-5 ps the transient spectra can be well fit with this three state model. The dynamics of both the low- and high-frequency regions of the spectrum consist of fast and slow processes. In the high-frequency region we observe the growth of a negative absorption change with a time constant 280±50 fs. This signal also shifts to higher frequencies, which is captured by the positive band at 3500 cm^{-1} in the spectrum of the first state (blue). This fast frequency shift represents the energy equilibration between the inner and outer hydration shells of the hydrated proton. The time constant is very similar to the previously found time constant of energy equilibration in small protonated clusters (260±40 fs).[4] The second state (green) decays more slowly to the final thermal state. This decay is due to heat energy transfer from the water phase of the nanodroplet to the surfactant molecules and the oil phase. These dynamics are non-exponential and therefore cannot be precisely fitted with our model (see discrepancy between the fit and experimental data at 5 ps in Figure 2). The time constant of this slow process depends on the size of nanodroplet and the delay time range considered (up to 5 ps or 20 ps) and is typically in the range of 1-5 ps. Similar energy equilibration dynamics have also been observed for proton hydration structures in cationic reverse micelles.[1]

4. Proton solvation in solutions of ethanesulfonic acid

To further investigate the nature of the bands at 2250 and 2600 cm^{-1} in the transient spectra of anionic reverse micelles, we also studied concentrated solutions of ethanesulfonic acid ($EtSO_3H$) in water. Concentrated solutions of ethanesulfonic acid resemble the interface of AOT-stabilized nanodroplets having a high concentration of sulfonate groups, protons and hydrophobic groups. In Figure S5 we show FTIR spectra of solutions with different concentrations of $EtSO_3H$ normalized to the absorption at 1725 cm^{-1}, which is attributed to the OH-bending vibration of hydrated protons.

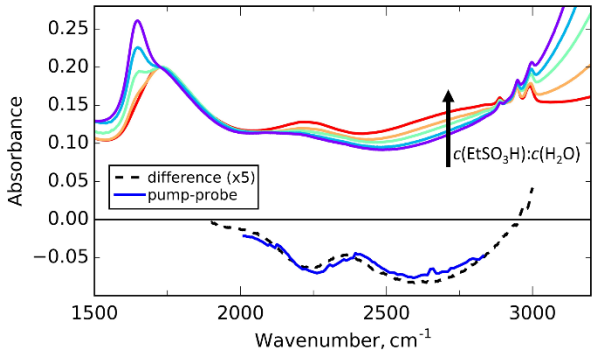

Figure S5. FTIR spectra of $EtSO_3H$ aqueous solutions with molar ratios $c(EtSO_3H)$:$c(H_2O)$ of 1:10; 1:8; 1:5; 1:3; 1:2 (colors from purple to red). The spectra are normalized with respect to the absorption of the bending vibration of hydrated proton at 1750 cm^{-1}. The black dashed line represents the difference between the FTIR spectra of [1:3] and [1:2] solutions, and the blue line compare represents the early delay time pump-probe spectrum of protons solvated in w_0=1 AOT microemulsion.

In these spectra we observe for all studied concentrations a broad continuous absorption in the 2000-3000 cm^{-1} frequency range. On top of this broad absorption we observe a band centered at ~2250 cm^{-1} which disappears upon dilution of the acid. Already at a molar ratio $EtSO_3H$:H_2O=1:2, ethanesulfonic acid is completely dissociated, as demonstrated by the vanishing of the $\nu_{as}(SO_2)$ and ν(S-O) absorption peaks at 1344 cm^{-1} and 904 cm^{-1} respectively[7] (Figure S6). Hence, the 2250 cm^{-1} band cannot be assigned to the OH-stretch vibration of undissociated ethanesulfonic acid. This band cannot also be the result of hydrogen-bonded dimer formation, since dimers of $EtSO_3H$ would likely also be present in neat $EtSO_3H$, and the spectrum of neat $EtSO_3H$ does not contain this band. Instead, this band can be assigned to the OH stretch vibration of a hydrogen-bonded proton solvation structure involving a sulfonate group. The gradual decrease of the 2250 cm^{-1} absorption band with increasing acid dilution indicates that the proton solvation environment changes. At the lowest studied molar fraction of ethanesulfonic acid (1:10), the 2250 cm^{-1} absorption is strongly suppressed resulting in a flat and broad absorption in the 2000-3000 cm^{-1} frequency range. At this concentration, due to the high excess of water, protons are fully solvated by water molecules and are well separated from the

ethanesulfonate anions. Conversely, at high ethanesulfonate concentrations the formation of ion pairs is highly probable.

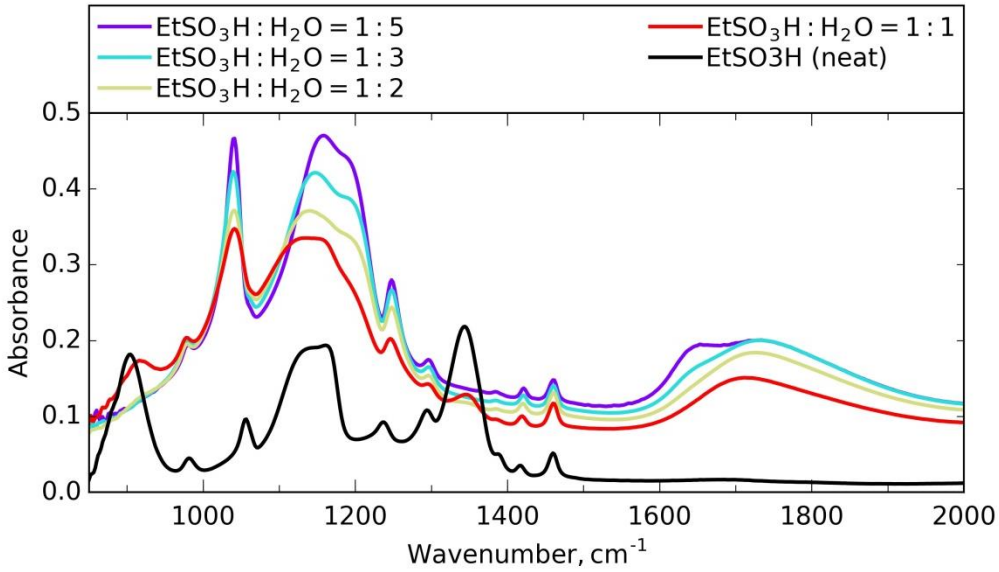

Figure S6. Infrared absorption spectra of ethanesulfonic acid solutions of different $EtSO_3H/H_2O$ molar ratio and of neat $EtSO_3H$. The spectra are normalized with respect to the absorption of the CH_2-bending vibration of ethanesulfonic acid at 1460 cm^{-1}.

The 2250 cm^{-1} absorption band does not represent undissociated $EtSO_3H$ or fully hydrated $H^+(H_2O)_n$, but a heteromolecular proton solvation complex $[RSO_3^-–H_3O^+(H_2O)_n]$. Interestingly, from the amplitudes $\nu_{as}(SO_2)$ and ν(S-O) absorption peaks at low water content ($EtSO_3H:H_2O$=1:1) we can conclude that only ~15% of the sulfonic acid remains undissociated. The 85% degree of ionization of ethanesulfonic acid also correlates with the concentration dependence of the characteristic hydrated proton bending absorption at 1750 cm^{-1}. This high degree of dissociation is in qualitative agreement with the results of an earlier 1H NMR study of methanesulfonic acid, in which 50% deprotonation at a 1:1 ratio was observed.[8] To facilitate sulfonic acid dissociation the water molecule accepting the proton has to be hydrogen bonded to two water molecules in order to become polarized and therefore to be basic enough.[9,10] It is possible that at low water content, the role of the two additional polarizing water molecules fulfilled by SO-groups of other sulfonate groups. In this case the proton solvation structure can be an asymmetric H_3O^+ ion with two or even three OH-groups strongly hydrogen bonded to sulfonate SO-groups.[11]

It is remarkable, that the transient absorption spectrum following excitation of the OH-vibrations of solvated proton structures in small AOT reverse micelles closely resembles the difference between FTIR spectra of ethanesulfonic acid solutions with low and high concentrations of the acid (Figure S5). This indicates that the excitation of small AOT nanodroplets results in a similar change of the proton-solvation structures as the dilution of ethanesulfonic acid solutions. This change is likely a bleaching of the OH stretch aborption bands of $[RSO_3^-–H_3O^+(H_2O)_n]$ solvation complexes, in the case of excitation of the AOT micelles as a result of weakening or partial dissociation of the hydrogen bonds due to local

heating, in the case of dilution of the ethanesulfonic acid solutions by replacing the $EtSO_3^-$ group by H_2O.

5. Transient absorption and anisotropy data

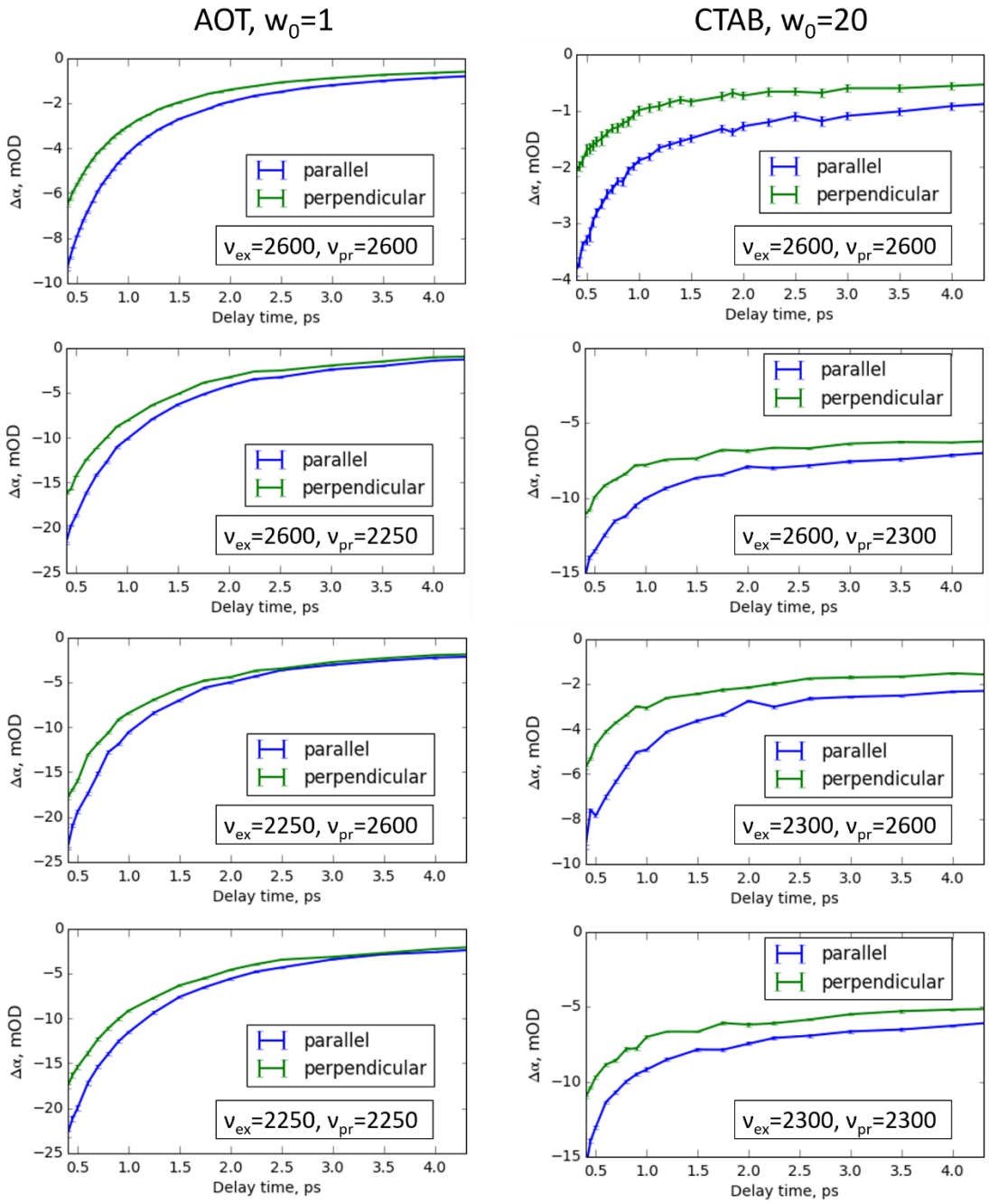

Figure S7. Example of transient absorption data for AOT and CTAB reverse micelles measured in parallel in perpendicular polarization configuration. The shown data are obtained by averaging of raw data over multiple pixels around the probe frequency (see Experimental methods). The lines connect the data points for better visualisation.

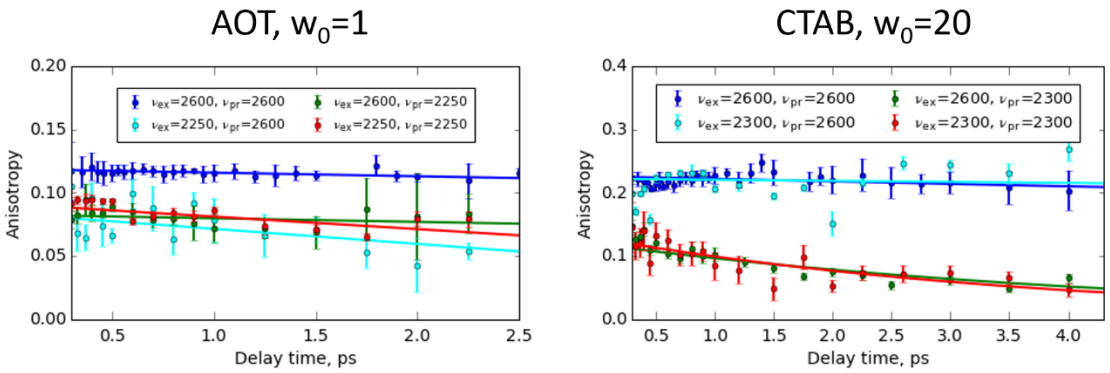

Figure S8. Example of anisotropy dynamics data obtained for AOT and CTAB reverse micelles. Such data, obtained for each reverse micelle system, were used to obtain the R_0 points shown in Figure 4. The lines represent exponential fits to the data.

References

(1) Sofronov, O. O.; Bakker, H. J. Slow Proton Transfer in Nanoconfined Water. *ACS Cent. Sci.* **2020**, *6*, 1150–1158.

(2) Cringus, D.; Bakulin, A.; Lindner, J.; Vöhringer, P.; Pshenichnikov, M. S.; Wiersma, D. A. Ultrafast Energy Transfer in Water−AOT Reverse Micelles. *J. Phys. Chem. B* **2007**, *111* (51), 14193–14207.

(3) Kinugasa, T.; Kondo, A.; Nishimura, S.; Miyauchi, Y.; Nishii, Y.; Watanabe, K.; Takeuchi, H. Estimation for Size of Reverse Micelles Formed by AOT and SDEHP Based on Viscosity Measurement. *Colloids Surfaces A Physicochem. Eng. Asp.* **2002**, *204* (1–3), 193–199.

(4) Sofronov, O. O.; Bakker, H. J. Vibrational Relaxation Dynamics of the Core and Outer Part of Proton-Hydration Clusters. *J. Phys. Chem. B* **2019**, *123* (29), 6222–6228.

(5) Woutersen, S.; Bakker, H. J. Ultrafast Vibrational and Structural Dynamics of the Proton in Liquid Water. *Phys. Rev. Lett.* **2006**, *96*, 138305.

(6) Dahms, F.; Costard, R.; Pines, E.; Fingerhut, B. P.; Nibbering, E. T. J.; Elsaesser, T. The Hydrated Excess Proton in the Zundel Cation H 5 O 2 + : The Role of Ultrafast Solvent Fluctuations. *Angew. Chemie Int. Ed.* **2016**, *55* (36), 10600–10605.

(7) Covington, A. K.; Thompson, R. Ionization of Moderately Strong Acids in Aqueous Solution. Part III. Methane-, Ethane-, and Propanesulfonic Acids at 25°C. *J. Solution Chem.* **1974**, *3* (8), 603–617.

(8) Telfah, A.; Majer, G.; Kreuer, K. D.; Schuster, M.; Maier, J. Formation and Mobility of Protonic Charge Carriers in Methyl Sulfonic Acid-Water Mixtures: A Model for Sulfonic Acid Based Ionomers at Low Degree of Hydration. *Solid State Ionics* **2010**, *181* (11–12), 461–465.

(9) Paddison, S. J. The Modeling of Molecular Structure and Ion Transport in Sulfonic Acid Based Ionomer Membranes. *J. New Mater. Electrochem. Syst.* **2001**, *4* (4), 197–207.

(10) Ishimoto, T.; Ogura, T.; Koyama, M. Stability and Hydration Structure of Model Perfluorosulfonic Acid Compound Systems, CF3SO3H(H2O)n (N=1-4), and Its Isotopomer by the Direct Treatment of H/D Nuclear Quantum Effects. *Comput. Theor. Chem.* **2011**, *975* (1–3), 92–98.

(11) Stoyanov, E. S.; Kim, K. C.; Reed, C. A. A Strong Acid That Does Not Protonate Water. *J. Phys. Chem. A* **2004**, *108* (42), 9310–9315.